Published in final edited form as:
Magn Reson Imaging. 2013 September ; 31(7): 1051–1058. doi:10.1016/j.mri.2013.03.011.

Feasibility of Coronary Artery Wall Thickening Assessment in Asymptomatic Coronary Artery Disease using Phase-Sensitive Dual Inversion Recovery MRI at 3T

Ahmed M. Gharib, MD, **Homeira Zahiri, MD**, **Jatin Matta, PA**, **Roderic I. Pettigrew, PhD, MD**, and **Khaled Z. Abd-Elmoniem, PhD**
Biomedical and Metabolic Imaging Branch, The National Institute of Diabetes and Digestive and Kidney Diseases, National Institutes of Health, Bethesda, Maryland, United States

Abstract

Objectives—The purpose of this study is to (1) investigate the image quality of phase-sensitive dual inversion recovery (PS-DIR) coronary wall imaging in healthy subjects and in subjects with known coronary artery disease (CAD) and to (2) investigate the utilization of PS-DIR at 3T in the assessment of coronary artery thickening in subjects with asymptomatic but variable degrees of CAD.

Materials and Methods—A total of 37 subjects participated in this Institutional Review Board approved and HIPAA-compliant study. These included 21 subjects with known CAD as identified on Multi-Detector CT angiography (MDCT). Sixteen healthy subjects without known history of CAD were included. All subjects were scanned using free-breathing PS-DIR MRI for the assessment of coronary wall thickness at 3T. Lumen-tissue contrast-to-noise ratio (CNR), signal-to-noise (SNR), and quantitative vessel parameters including lumen area and wall thickness were measured. Statistical analyses were performed.

Results—PS-DIR was successfully completed in 76% of patients and in 88% of the healthy subjects. Phase-sensitive signed magnitude reconstruction, compared to modulus magnitude images, significantly improved lumen-tissue contrast-to-noise ratio (CNR) in both healthy subjects (26.73±11.95 vs. 14.65±9.57, $p<0.001$) and in patients (21.45±7.61 vs. 16.65±5.85, $p<0.001$). There was no difference in image CNR and SNR between groups. In arterial segments free of plaques, coronary wall was thicker in patients in comparison to healthy subjects (1.74±0.27mm vs. 1.17±0.14mm, $p<0.001$) without a change in lumen area (4.51±2.42 mm^2 vs. 5.71±3.11 mm^2, $p=0.25$).

Conclusions—This is the first study to demonstrate the feasibility of successfully obtaining vessel wall images at 3T using PS-DIR in asymptomatic patients with known variable degrees of CAD as detected by MDCT. This was achieved with a fixed subject-invariant planning of blood signal nulling. With that limitation alleviated, PS-DIR coronary wall MRI is capable of detecting arterial thickening and positive arterial remodeling at 3T in asymptomatic CAD.

Address for correspondence: Khaled Z. Abd-Elmoniem PhD., National Institutes of Health, Clinical Research Center, Bldg.10, Rm. 3-5340, MSC 1263, 10 Center Drive, Bethesda, MD 20892, Tel: (301)451-4340, Fax: (301)496-9933, abdelmoniemkz@mail.nih.gov.

Keywords

Atherosclerosis; coronary artery imaging; vessel wall; black blood MRI; Phase sensitive; dual inversion recovery; 3T

Introduction

Latest advancements in coronary Magnetic Resonance Angiography (MRA) at 1.5T and 3T allowed for the non-invasive assessment of coronary artery disease without the need for radiation (1–6). These techniques have been focusing on the assessment of luminal narrowing. However, thickening or arterial remodeling of the vessel wall often precedes luminal narrowing of the coronary arteries (7–9). Intravascular ultrasound (IVUS) has often been used as the reference standard of coronary vessel wall evaluation and to evaluate the effect of therapy (10). The invasive nature of this technique is an obvious limiting factor against extensive use in early coronary plaque characterization. Hence, early atherosclerotic arterial wall changes that could be modulated by appropriate therapy are usually obscured or underestimated by conventional coronary angiography, non-invasive Multi-Detector Computer Tomography (MDCT) angiography or MRA techniques. Therefore, the need for a non-invasive means for coronary arterial wall evaluation has resulted in the development of several MR methods (11–17). Although these techniques have shown promise in evaluating patients with coronary artery disease (CAD), they have been mainly performed using 1.5T MRI scanners, time-consuming, and/or mandating a considerably large set of imaging parameters. The increasing availability of higher field strength scanners with the promise of higher SNR and the potential for shorter acquisition times, therefore, necessitates alterations of these techniques (18). Optimization of these intricate coronary vessel wall MR sequences requires the development of short breath hold or free-breathing imaging protocols for patient convenience and improved success rate. In addition, optimization requires reducing amount of interaction needed from the operator by reducing the number of the manually-adjusted exam parameters. These MR sequences, therefore, need to tackle the challenges of ideal blood pool nulling and fat suppression consistently during the diastole rest period of least cardiac motion. Such challenges are accentuated at 3T mainly due to larger B_0 and B_1 inhomogeneities, and consequently shorter T_2^* compounded by the difference in inversion time due to the prolonged T_1 at higher field strength compared to 1.5T (18). Some of these challenges have been addressed by using improved motion-sensitized driven equilibrium (iMSDE) at 3T (19) to obtain homogeneous blood pool suppression or by using adiabatic inversion sequences (20). An alternative technique was to use phase-sensitive dual inversion recovery (PS-DIR) at 3T (21). Previous DIR-based vessel wall imaging techniques require subject-specific heart-rate-sensitive inversion nulling time (TI^*) to suppress the blood signal. On the other hand, PS-DIR utilizes a fixed subject- and heart-rate invariant inversion time (TI), thereby, is less operator-dependent and less sensitive to subjects' natural heart rate variability. This is achieved by using the phase-map of the acquired data to suppress blood signal artifacts and to restore the contrast between vessel lumen and wall. Previous studies that compared breath-hold PS-DIR to conventional DIR imaging in healthy subjects demonstrated a good agreement in vessel wall thickness as well as a significant improvement in lumen-wall CNR relative to standard DIR (21). Unlike the studies performed at 1.5T, the feasibility of these methods at 3T was primarily demonstrated in healthy subjects (18, 19, 21–24). To date only two studies (25, 26) utilized 3T vessel wall imaging to study subjects with CAD risk factors (25) or known CAD (26). However, these studies included subject with only risk factors for CAD and no other documentation of disease (25) or a preselected group with only <50% stenotic lesions(26). None were utilized successfully for imaging subjects with documented CAD of varying degrees that would present the gamut of associated challenges. Such patients present additional challenges due

to their variable heart rates, blood flow changes due to the variability of multiple CAD lesions, body habitus, and/or inability to sustain breath-holds. All these may further influence the magnetization steady state and thereby the black blood image quality. The purpose of this study is to optimize a fast free-breathing coronary arterial wall imaging sequence using PS-DIR to omit the need to identify the blood signal nulling time for each subject and investigate its ability for the assessment of coronary artery thickening at 3T in patients with known asymptomatic but documented CAD of variable severity in comparison to control subjects without known history of CAD.

PS-DIR Imaging and Reconstruction

A conventional dual inversion-recovery (DIR) preparation pulse as shown in Figure 1a consists of a non-selective inversion directly followed by a slice-selective re-inversion of the magnetization at the anatomical level of interest. This prepulse maintains the original magnetization at the anatomical level while the inverted magnetization of the in-flowing blood is nulled at a specific nulling time TI* (27). Imaging vessel wall at time TI* requires accurate determination of TI* which depends on and is sensitive to heart rate, cardiac motion, and the complexity of the in-flowing blood specific path. The loss of the MR signal polarity in typical DIR black-blood images may result in a suboptimal blood-tissue contrast if the imaging time TI ≠ TI* (21, 28). Independently, another timing parameter, trigger time (TD) has to be set to trigger imaging during the period of minimal myocardial motion in order to reduce the adverse effects of intrinsic myocardial motion (4, 29, 30).

In contrary to DIR, phase-sensitive DIR black-blood imaging (21) as shown in Figure 1b alleviates the need to suppress blood signal and the conflicting requirements for arranging for the null to occur in diastole. PS-DIR, therefore, does not null or suppress the blood signal but allows for the inverted magnetization blood signal to be distinguished from the non-inverted signal from the vessel wall and other tissues based on its image complex phase during post-processing and phase-sensitive reconstruction. During reconstruction, a ring-shaped region of interest (ROI) is selected around the location of the coronary artery. The background inhomogeneity phase map in and around the artery is estimated using a previously described region-growing algorithm (21, 31). The inhomogeneity phase is subtracted from the total phase and the result is multiplied by the original modulus magnitude image in order to obtain a signed magnitude image. To avoid detrimental effect of multiple phase wrappings, the region growing algorithm runs only locally in close proximity to the coronary artery. The small localized processing substantially minimizes the ambiguity associated with phase-wrapping that may otherwise fail the technique if the whole image was analyzed.

Methods

A total of 37 subjects were prospectively included and signed informed consent to participate in this Institutional Review Board approved and HIPAA-compliant study. The subjects were divided into two body-mass-index (BMI) matched groups. The first group included 21 subjects with at least one Framingham CAD risk factors and the second group included 16 healthy subjects without known history and/or risk factors for CAD. Both groups were scanned in the supine position using a commercial human 3T system (Achieva, Philips Medical Systems, Best, NL). A 32-channel phased array cardiac receiver coil and vector ECG triggering (VCG) were utilized (32). All 21 subjects with CAD risk factors were asymptomatic and had a coronary MDCT. With the lack of CAD history or risk factors that would justify radiation exposure, the 16 healthy subjects did not have a coronary MDCT scan.

Multi-Detector Computer Tomography

All 21 patients had at least one risk factor for CAD and known CAD based on MDCT scans interpreted as positive for coronary lesions. The patients had MDCT scans using a 320-detector scanner (Aquilion ONE; Toshiba Medical Systems, Tochigiken, Japan) in 2 patients, 6 patients with 256-detector scanner (Brilliance iCT, Philips, Eindhoven, The Netherlands) and 64-detector scanner (DEFINITION, Siemens Health Care, Forchheim, Germany) in the remaining 13 patients. The MR scans were obtained within an average of 43 days of the MDCT scans.

The MDCT protocol was similar to previously described techniques using identical equipment (33–36). Briefly, 50–100mg of oral metoprolol was given 60 minutes prior to MDCT when the patients' heart rate needed to be lowered below 65 beats per minute (37). All subjects were in sinus rhythm and none had atrial fibrillation. MDCT was performed using a tube voltage of 120 kV and current of 400–580 mAs with a 220mm field of view, 512 matrix and retrospective ECG gating for the 64 detectors scanner. Retrospective gating was needed when the patients' heart rate was above 65bpm. Prospective gating was used for the remaining patients imaged on the 256 and 320 detector scanners. For contrast, 70–80 ml of non-ionic contrast (Isovue, Bracco Diagnostic Inc, Princeton, NJ) was injected through an 18–20 gauge peripheral venous access at a rate of 4–5 ml / sec followed by 50 ml of normal saline at the same injection rate.

MDCT Post Processing and Analysis

For the MDCT studies, image post processing, analysis and interpretation were performed using a three dimensional software tool (AZE, Tokyo, Japan). Images were evaluated for the presence of disease with a binary grading of its severity (greater or less than 50% stenosis). For this grading, MDCT coronary artery images were assessed in consensus by two blinded readers for the presence of CAD and a categorical degree of coronary artery stenosis. The degree of stenosis was classified as mild (<50% stenosis) or moderate to severe (>50% stenosis) (38). The degree of stenosis on MDCT was assessed by area reduction of the coronary artery lumen.

MRI Scout Scanning

Localization of the heart and the right coronary artery (RCA) for all the subjects was performed similar to previously published methodologies (11, 39). A free-breathing axial VCG-triggered, steady-state free precession cine image series was acquired (TE/TR/α=1.8ms/3.8ms/45°, and a temporal resolution of 39.6ms) at the proximal to mid RCA. The patient-specific time-delay (TD) between the R-wave of the ECG and the diastolic rest period was visually identified from the cine image and used for the subsequent coronary MRA and wall imaging.

Coronary MRA

Volume-targeted respiratory navigator-gated 3D segmented k-space gradient echo coronary MRA was acquired using the previously identified TD. The coronary MRA was oriented in parallel to the major axis of the RCA system with TE/TR/α=2.1ms/8ms/20°, FOV=270×270×45mm^3, matrix=384×270×15, and acquired voxel size of 0.7×1×3mm^3. Navigator respiratory gating was performed utilizing a 5mm gating window and slice tracking (40, 41).

Coronary Arterial Wall MRI

Single-slice PS-DIR spiral gradient echo coronary vessel wall images were acquired using a fixed subject-invariant inversion time TI=200ms. Datasets were acquired using a segmented

k-space spiral acquisition with spectral spatial water-selective excitation (42). The spiral readout consisted of 20 interleaves with a flip angle α=45°, an acquisition window of 20ms, TE/TR=2.1ms/1RR interval, and the spatial resolution was $0.69\times0.69\times8.0mm^3$ (FOV = $200\times200\times8mm^3$, matrix = 288×288×1). The re-inversion slice thickness of 15mm was used to accommodate for potential spatial mis-registration between the magnetization-prepared slab and the imaged slice due to through-plane cardiac motion. Data were acquired during free breathing using respiratory navigator gating (41). The navigator was localized at the lung-liver interface of the right hemi-diaphragm with a 3mm gating window and a correction factor of 0.6 in superior-inferior direction (43). Immediately after dual-inversion, a navigator restore pulse (44) was used to optimize navigator performance. The vessel wall image was acquired at the proximal or proximal aspect of mid RCA segments at a location without tortuosity, and without obvious plaque or narrowing. This was obtained in a plane perpendicular to the long axis of the targeted vessel segment.

The collected phase and magnitude data were used to reconstruct phase-sensitive signed-magnitude images that were then used in all later analyses as described in previous literatures (21).

MRI Data Analysis

All images were randomized, anonymized, and scored by two observers in consensus for the visual quality of the vessel wall according to the ability to distinguish the wall from surrounding structures. A score from 0–4, using criteria as previously described (45), was assigned to each image. A score of 0 indicated an undistinguishable coronary wall; a score of 1 (poor) indicated the coronary artery wall partly visible (<50%) with incomplete borders; 2 (fair), where 50%–75% of the coronary artery wall is visible and distinguishable from the lumen and surroundings; 3 (good), where the coronary artery wall is mostly distinguishable with only small portions of the vessels (<25%) not present; and 4 (excellent), where the coronary artery wall is completely visible with sharply defined borders. The consensus of the two observers' scores determined the final assessment of image quality and an image with a good or excellent quality was considered adequate for quantitative analysis. These images were all pooled and analyzed, blinded to subject information.

Coronary Wall Measurement

Image processing was performed off-line on a personal computer using an in-house developed software tool using Matlab® ver. 7.8 (Mathworks, Natick, MA). A semi-automatic algorithm for wall thickness measurement was developed based on the work of Botnar et al. (46). Briefly, images were zoomed to 500% and the center of the vessel wall was manually traced as an initial localization step. Then, a one-dimensional Gaussian-shape model was automatically fit across the wall at all points along the wall centerline. The outer and inner boundaries of the coronary wall were automatically identified as the two points of steepest gradients on the sides of each of the Gaussian shapes. Coronary artery wall thickness in each image was measured as the average distance between the previously identified inner and outer boundaries along the wall circumference. Lumen area (LA) and outer wall area (OW) are the areas of the regions surrounded by the inner and the outer boundaries of the vessel, respectively. Vessel wall area (W) is the difference between the outer wall area and the lumen area (OW-LA). The ratio W/OW equals the ratio between vessel wall area to the outer wall area.

Additionally, in order to compensate for the age difference between the healthy and the CAD groups, age-adjusted wall thickness values were calculated for the healthy subject group following the results of the previous study by Scott AD et al. (47) according to the formula $\mathrm{Wa}=\mathrm{Wm}+0.0088\,(\overline{\mathrm{Age}}_{\mathrm{CAD}}-\overline{\mathrm{Age}}_{H})$. Here, Wa, measured in millimeters (mm), is the

age-adjusted wall thickness for a healthy subject, Wm (mm) is the measured wall thickness for a healthy subject, and $\overline{\mathrm{Age}}_{H}$ and $\overline{\mathrm{Age}}_{\mathrm{CAD}}$ measured in years, are the average ages of the healthy and CAD subject groups, respectively.

Lumen-wall CNR was calculated from the PS-DIR signed-magnitude and from the modulus-magnitude-only images, and SNR was calculated from the PS-DIR signed magnitude images using the formula previously reported (21) where noise standard deviation was measured in a circular region of interest (diameter=25mm) in the lungs where no anatomical structures could be visually identified. This was performed for both groups (CAD and healthy subjects).

Unpaired two-tails Student t-test was used to compare all measurements between healthy and CAD subjects. Paired two-tails Student t-test was used to compare lumen-wall CNR using signed-magnitude PS-DIR data versus using only modulus-magnitude data. MedCalc® version 11.6 (MedCalc Software, Mariakerke, Belgium) was used for all statistical analyses. A p value of <0.05 was considered to be statistically significant. Measurements are represented as mean values ± 1 standard deviation except mentioned otherwise.

Results

MDCT image quality was excellent to good for all CAD subjects (48). All these subjects demonstrated at least one vessel involvement with atherosclerotic disease with varying degrees of narrowing. The average Agatston calcium score was 342.5 (±610.3) and 12/21 patients had at least one lesion that was >50% stenosed indicating variability of CAD in this group. The CAD subjects' demographics, calcium score, and MDCT findings are displayed in table 1 using a modified 17-segment American Heart Association model of the coronary vessels(49). There was no statistically significant difference between CAD and healthy subjects' BMI (patients: 28.0±3.7, healthy: 27.2±5.1, p=NS) or ratio of male to female. However, the healthy subjects were statistically significantly younger than the CAD group (29.8±6.9 years vs. 58.9±10.8 years, $p<0.001$). This age difference was inevitable since healthy subjects were chosen based on absence of known history of CAD and/or risk factors, which is usually affected by age.

PS-DIR was successfully completed in all subjects. Average navigator acceptance rate was 15% and average scan duration was 80s. Image quality scores are listed in Table 2. Adequate image quality for analysis was scored in 76% and in 88% of the CAD and the healthy subjects, respectively. The vessel wall images for two healthy controls and five CAD subjects were discarded due to poor ECG quality or subject motion. Examples of healthy and CAD images are demonstrated in Figure 2. Vessel measurements are summarized in Table 3 and in Figure 3. In particular, at the locations without noticeable plaques or narrowing on the RCA MRA, there was no difference in lumen area between healthy and CAD subjects (healthy: 4.51±2.42 mm^2 vs. CAD: 5.71±3.11 mm^2, p=0.25), confirming the visual criteria used for selecting the anatomical location for imaging. Meanwhile, coronary wall thickness was thicker in CAD in comparison to healthy subjects (CAD: 1.74±0.27mm vs. healthy: 1.17±0.14 mm, $p<0.0001$). Wall thickening remained significantly thicker even after age-adjustment of the healthy subject measurements (CAD: 1.74±0.27 mm vs. age-adjusted healthy: 1.42±0.14 mm, $p<0.001$). Wall area (W), outer wall area (OW), and the ratio W/OW were all increased significantly as shown in Table 3.

CNR improved significantly when both the phase and the magnitude were used to construct signed magnitude images compared to modulus-magnitude images, see Figure 4. In healthy subjects the increase in CNR was (26.72±11.95 vs. 14.65±9.57, p=0.0003) while in the CAD group the increase in CNR was (21.45±7.61 vs. 16.64± 5.85, p=0.003). There was no inter-

group difference in PS-DIR SNR (26.65±7.68 vs. 26.13±12.82, p=NS) and CNR (21.45±7.61 vs. 26.73±11.95, p=NS).

Discussion

Phase-sensitive DIR imaging was utilized in this study for the first time to successfully develop and implement fast free-breathing coronary arterial wall imaging at 3T in subjects with known and variable degrees of CAD. PS-DIR acquisition and reconstruction overcome the effect of prolonged T1 of the blood at 3T, thereby, suppressing the blood signal using a fixed subject-invariant inversion time that is curtail in patients with variable degrees of CAD. This was achieved with success rates of 76% for CAD and 88% for healthy subjects. This success rate is within the range of 65–79% for previously described techniques at 1.5T performed consecutively in CAD patients (14–16). Other studies that evaluated coronary vessel wall in patients at 1.5T only included a small cohort of 5–6 CAD patients (11, 12). One study by Kim et al. (13) included a relatively small percentage of coronary vessel wall images (44%) of a larger group of 136 patients who were also assessed for plaque burden in the aorta. Their patient selection approach to include coronary vessel wall imaging at 1.5T might have contributed to their higher success rate of 88%. This success rate is also similar to results obtained at 3T when compared to single PS-DIR technique (25). However, this was tested in subjects with only risk factors of CAD (25) that do not exhibit the variability and more severe degrees of stenosis in our patient population. Hays et al. (26) studied a preselected patient poplutaion with documented CAD lesion that are <50% stenosed using a breath hold DIR technique that did not utilize PS methods. This preselection of their patient population precludes accurate assessment of the success rate. Both these studies (25, 26) performed at 3T tested their methods on patient populations with relatively lower BMI of approximate average of 25 compared to 28 (overweight) in our study. The paucity of such patient studies and relatively low success rate, even at a more homogenous 1.5T magnetic field, reflects the difficulty of determining the optimal set of imaging parameters to reliable blood signal nulling while suppressing breathing and heart motion-induced artifacts.

The use of PS-DIR instead of standard dual inversion method has alleviated the need for the previously required TI dependant blood pool nulling prepulses and the associated meticulous consideration of proper inversion time predictions in lieu of prolonged T1 time encountered at 3T and variability of coronary blood flow in patients with CAD. These requirements are in practice difficult to achieve given the complex blood pathways from the heart into the arteries and the complex blood exchange with the planned slices. The choice of TI=200ms is preferred to allow enough washing-out time for the blood that is in the imaged vessel segment during the dual inversion preparation pulse (21) especially with the potentially slow-flowing blood in patients.

The utilization of subject-invariant TI in combination with spiral imaging allowed for a short acquisition window of 20ms that can fit in a single RR interval and permits sharper motion-suppressed imaging even of patients with a short diastolic rest period. This is the shortest reported acquisition window at 3T or 1.5T that was applied with TR= 1 RR interval and utilized in imaging patients with CAD. The closest published methods at 3T using a 21ms acquisition window required repetition time of two heart beats (18) to obtain adequate blood signal nulling, SNR and CNR. To allow 3D imaging with a large volumetric coverage, repetition time of a single heart beat was predominantly utilized in 3D sequences in which TR=2 RR is not affordable due to the prohibitively long acquisition times (19, 20). The latter 3D sequences, therefore, are completed in long scan times ranging from 6–22 minutes. The need to acquire data after every other heart beat for TR=2 RR is no longer required as spiral PS-DIR allows short inversion time, short acquisition window, and high intrinsic lumen-wall CNR. These improvements allow a greater ability to image the vessel wall and a

short total scan time of approximately 1 minute and 20 seconds with 10–20% navigator efficiency for a heart rate of 70 beats per minute. All these factors, when combined, contributed to the high success rate and good image quality score representing adequate blood signal suppression. This study has demonstrated this achievement in both CAD and healthy subjects. A previous study (21) demonstrated the statistically significant improvement in wall-lumen CNR when using PS-DIR imaging versus conventional DIR in humans. Hence, building on this prior study, the presented experiments focused on the feasibility of using this new technique in patients with known CAD. Trading the improved PS-DIR lumen-vessel CNR for higher resolution data acquisition must be carefully investigated for multiple reasons. First, the SNR is major factor that is likely to worsen at higher resolution. Second, higher resolution will translate into longer acquisition, which will potentially blur and deteriorate the image quality.

Although the focus of this study was on 2D PS-DIR imaging, the technique can be extended to 3D image acquisition in a setup similar to the one previously published by Botnar et al. (17). Additionally, the vessel wall image was acquired at a location without obvious plaque or narrowing. In principle, coronary vessel wall imaging is possible in calcified regions. However, calcification may pose additional challenges due to its fast signal decay and potential susceptibility artifacts that might be accentuated in spiral imaging. The complete effect of calcification on PS-DIR imaging remains to be investigated.

PS-DIR black blood technique at 3T successfully differentiates coronary wall thickness between patients with variable CAD and healthy subjects at locations without noticeable plaques or stenosis, as was confirmed by absence of lumen area difference. Coronary wall thickness measured using PS-DIR was significantly thicker in CAD subjects compared to healthy controls even after adjusting for age difference. The current study further establishes the link between coronary vessel wall thickness and early atherosclerosis in subjects with asymptomatic CAD. The results using free-breathing PS-DIR at 3T and with subject-invariant inversion time compare favorably with measurements previously established at 1.5T using dual inversion recovery black blood MRI techniques for investigation of the coronary artery wall thickness (11–16). Our results demonstrated a slightly thicker vessel wall compared prior studies obtain in patients using 3T (25, 26). This is probably due to the more variable degree of disease compared to the other studies at 3T as indicated above.

Limitations

One of the study limitations is the relatively small number of subjects; however, this was sufficient to demonstrate for the first time the feasibility of accelerated PS-DIR coronary wall imaging technique at 3T in patients with known CAD. This is an initial step forward toward the assessment of stratification of CAD. Further studies with larger numbers of patient groups would be required for a more comprehensive assessment of the degree of CAD using this novel vessel wall imaging method. Another limitation is that this study did not explore the potential of improving spatial resolution that would be anticipated given the increased SNR at 3T. However, the presented in-plane spatial resolution of 0.69×0.69 mm^2 remains in the range of previous publications at 3T and 1.5T. The increased voxel size in this study was due to the increased slice thickness of 8mm which was the minimum thickness allowed when using spectral-spatial water-selective excitation pulses. This allowed for the necessary fat suppression during slice excitation without additional preparation pulses. Moreover, the imaged slices were carefully chosen perpendicular to a straight segment of the RCA. This slice thickness did not affect the ability of the technique in differentiating vessel wall thickness in patients with CAD from healthy controls. Imaging tortuous segments may require planning thinner slices. Thinner slices are possible if other fat suppression techniques are utilized such as prepulse fat saturation and conventional

excitation pulses. This however will potentially be associated with lower SNR. Nevertheless, compensation for the loss of SNR via multiple thin-slice averaging without compromising the measurement fidelity is doubtful due to the small caliper of the coronary arteries and the likelihood of signal blurring associated with averaging and thus would require further investigation and optimization. Although this study did not exploit the excess SNR at 3T to improve the spatial resolution but it did utilize this excess signal for reducing the temporal resolution and acquiring data at single RR interval repetition time while maintaining a good in-plane resolution of 0.69×0.69 mm^2. While the used resolution was enough to differentiate between the two groups, a shorter spiral readout might be advantageous in the future to improve actual resolution and overcome the short T_2* signal decay at 3T. Another potential limitation is the age mismatch between healthy and CAD subjects. This age difference was inevitable since healthy subjects were chosen based on the absence of known history of CAD and/or risk factors, which is usually affected by age. A prior study by Scott AD et al (47), reported an age-related vessel wall thickening using a vessel wall imaging method at 1.5T in 21 healthy subjects. However, the authors did not correlate this increased with Framingham CAD risk factors such as age >45 years old (6/21) and smoking history (7/21) which was present in their subject population. In our study we have included subjects with CAD not only based on CAD risk factors but also the confirmed presence of CAD on MDCT. Nonetheless, this potential age difference was accounted for in our study by mathematically adjusting for the proposed 0.088mm/decade increase in vessel wall thickness, with a preserved statically significant difference between the CAD and healthy subjects. Finally, the number of CAD patients was not sufficient to study the impact of severity of stenosis on vessel wall thickness, and the purpose of the study is to demonstrate the ability of this previously published method in differentiating patients with known and variable degrees of CAD on MDCTA and healthy subjects without known CAD risk factors. Further studies with larger patient populations might be useful to determine the impact of the degree of stenosis on vessel wall thickness.

Conclusions

This is the first study to demonstrate the feasibility of successfully obtaining vessel wall images at 3T using PS-DIR in asymptomatic patients with known and variable degrees of CAD. This presented method is less operator-dependent alleviating the need for subject-specific TI scan adjustments for coronary blood signal suppression. Additionally, this study presents the strength of PS-DIR at 3T and the capability of differentiating between the vessel wall thickness in these asymptomatic wide range of documented degree of CAD and healthy controls.

References

1. Kim WY, Danias PG, Stuber M, et al. Coronary magnetic resonance angiography for the detection of coronary stenoses. N Engl J Med. 2001; 345(26):1863–9. [PubMed: 11756576]
2. Sakuma H, Ichikawa Y, Suzawa N, et al. Assessment of coronary arteries with total study time of less than 30 minutes by using whole-heart coronary MR angiography. Radiology. 2005; 237(1): 316–21. [PubMed: 16126921]
3. Sommer T, Hackenbroch M, Hofer U, et al. Coronary MR angiography at 3.0 T versus that at 1.5 T: initial results in patients suspected of having coronary artery disease. Radiology. 2005; 234(3):718–25. [PubMed: 15665221]
4. Sakuma H, Ichikawa Y, Chino S, Hirano T, Makino K, Takeda K. Detection of coronary artery stenosis with whole-heart coronary magnetic resonance angiography. J Am Coll Cardiol. 2006; 48(10):1946–50. [PubMed: 17112982]

5. Yang Q, Li K, Liu X, et al. Contrast-enhanced whole-heart coronary magnetic resonance angiography at 3.0-T: a comparative study with X-ray angiography in a single center. J Am Coll Cardiol. 2009; 54(1):69–76. [PubMed: 19555843]
6. Gharib AM, Abd-Elmoniem KZ, Ho VB, et al. The feasibility of 350 mum spatial resolution coronary magnetic resonance angiography at 3 T in humans. Invest Radiol. 2012; 47(6):339–45. [PubMed: 22551651]
7. Glagov S, Weisenberg E, Zarins CK, Stankunavicius R, Kolettis GJ. Compensatory enlargement of human atherosclerotic coronary arteries. N Engl J Med. 1987; 316(22):1371–5. [PubMed: 3574413]
8. Libby P. Current concepts of the pathogenesis of the acute coronary syndromes. Circulation. 2001; 104(3):365–72. [PubMed: 11457759]
9. Libby P. Coronary artery injury and the biology of atherosclerosis: inflammation, thrombosis, and stabilization. Am J Cardiol. 2000; 86(8B):3J–8J. discussion J–9J.
10. Nissen SE, Tuzcu EM, Schoenhagen P, et al. Effect of intensive compared with moderate lipid-lowering therapy on progression of coronary atherosclerosis: a randomized controlled trial. JAMA. 2004; 291(9):1071–80. [PubMed: 14996776]
11. Botnar RM, Stuber M, Kissinger KV, Kim WY, Spuentrup E, Manning WJ. Noninvasive coronary vessel wall and plaque imaging with magnetic resonance imaging. Circulation. 2000; 102(21): 2582–7. [PubMed: 11085960]
12. Fayad ZA, Fuster V, Fallon JT, et al. Noninvasive in vivo human coronary artery lumen and wall imaging using black-blood magnetic resonance imaging. Circulation. 2000; 102(5):506–10. [PubMed: 10920061]
13. Kim WY, Astrup AS, Stuber M, et al. Subclinical coronary and aortic atherosclerosis detected by magnetic resonance imaging in type 1 diabetes with and without diabetic nephropathy. Circulation. 2007; 115(2):228–35. [PubMed: 17190865]
14. Miao C, Chen S, Macedo R, et al. Positive remodeling of the coronary arteries detected by magnetic resonance imaging in an asymptomatic population: MESA (Multi-Ethnic Study of Atherosclerosis). J Am Coll Cardiol. 2009; 53(18):1708–15. [PubMed: 19406347]
15. Terashima M, Nguyen PK, Rubin GD, et al. Right coronary wall CMR in the older asymptomatic advance cohort: positive remodeling and associations with type 2 diabetes and coronary calcium. J Cardiovasc Magn Reson. 2010; 12:75. [PubMed: 21192815]
16. Macedo R, Chen S, Lai S, et al. MRI detects increased coronary wall thickness in asymptomatic individuals: the multi-ethnic study of atherosclerosis (MESA). J Magn Reson Imaging. 2008; 28(5):1108–15. [PubMed: 18837001]
17. Botnar RM, Kim WY, Bornert P, Stuber M, Spuentrup E, Manning WJ. 3D coronary vessel wall imaging utilizing a local inversion technique with spiral image acquisition. Magn Reson Med. 2001; 46(5):848–54. [PubMed: 11675634]
18. Peel SA, Hussain T, Schaeffter T, Greil GF, Lagemaat MW, Botnar RM. Cross-sectional and In-plane coronary vessel wall imaging using a local inversion prepulse and spiral read-out: A comparison between 1.5 and 3 tesla. J Magn Reson Imaging. 2011
19. Wang J, Gerretsen SC, Maki JH, et al. Time-efficient black blood RCA wall imaging at 3T using improved motion sensitized driven equilibrium (iMSDE): feasibility and reproducibility. PLoS One. 2011; 6(10):e26567. [PubMed: 22028910]
20. Priest AN, Bansmann PM, Kaul MG, Stork A, Adam G. Magnetic resonance imaging of the coronary vessel wall at 3 T using an obliquely oriented reinversion slab with adiabatic pulses. Magn Reson Med. 2005; 54(5):1115–22. [PubMed: 16206145]
21. Abd-Elmoniem KZ, Weiss RG, Stuber M. Phase-sensitive black-blood coronary vessel wall imaging. Magn Reson Med. 2010; 63(4):1021–30. [PubMed: 20373403]
22. Priest AN, Bansmann PM, Mullerleile K, Adam G. Coronary vessel-wall and lumen imaging using radial k-space acquisition with MRI at 3 Tesla. European radiology. 2007; 17(2):339–46. [PubMed: 17021711]
23. Koktzoglou I, Simonetti O, Li D. Coronary artery wall imaging: initial experience at 3 Tesla. J Magn Reson Imaging. 2005; 21(2):128–32. [PubMed: 15666403]

24. Botnar RM, Stuber M, Lamerichs R, et al. Initial experiences with in vivo right coronary artery human MR vessel wall imaging at 3 tesla. J Cardiovasc Magn Reson. 2003; 5(4):589–94. [PubMed: 14664136]
25. Abd-Elmoniem KZ, Gharib AM, Pettigrew RI. Coronary Vessel Wall 3-T MR Imaging with Time-resolved Acquisition of Phase-Sensitive Dual Inversion-Recovery (TRAPD) Technique: Initial Results in Patients with Risk Factors for Coronary Artery Disease. Radiology. 2012
26. Hays AG, Kelle S, Hirsch GA, et al. Regional coronary endothelial function is closely related to local early coronary atherosclerosis in patients with mild coronary artery disease: pilot study. Circulation. 2012; 5(3):341–8. [PubMed: 22492483]
27. Fleckenstein JL, Archer BT, Barker BA, Vaughan JT, Parkey RW, Peshock RM. Fast short-tau inversion-recovery MR imaging. Radiology. 1991; 179(2):499–504. [PubMed: 2014300]
28. Xie J, Bi X, Fan Z, et al. 3D flow-independent peripheral vessel wall imaging using T(2)-prepared phase-sensitive inversion-recovery steady-state free precession. J Magn Reson Imaging. 2010; 32(2):399–408. [PubMed: 20677269]
29. Spuentrup E, Stuber M, Botnar RM, Manning WJ. The impact of navigator timing parameters and navigator spatial resolution on 3D coronary magnetic resonance angiography. Journal of magnetic resonance imaging : JMRI. 2001; 14:311–8. [PubMed: 11536409]
30. Stuber M, Weiss RG. Coronary magnetic resonance angiography. J Magn Reson Imaging. 2007; 26(2):219–34. [PubMed: 17610288]
31. Szumowski J, Coshow WR, Li F, Quinn SF. Phase unwrapping in the three-point Dixon method for fat suppression MR imaging. Radiology. 1994; 192(2):555–61. [PubMed: 8029431]
32. Fischer SE, Wickline SA, Lorenz CH. Novel real-time R-wave detection algorithm based on the vectorcardiogram for accurate gated magnetic resonance acquisitions. Magn Reson Med. 1999; 42(2):361–70. [PubMed: 10440961]
33. Achenbach S, Ropers D, Kuettner A, et al. Contrast-enhanced coronary artery visualization by dual-source computed tomography--initial experience. Eur J Radiol. 2006; 57(3):331–5. [PubMed: 16426789]
34. Rybicki FJ, Otero HJ, Steigner ML, et al. Initial evaluation of coronary images from 320-detector row computed tomography. Int J Cardiovasc Imaging. 2008; 24(5):535–46. [PubMed: 18368512]
35. de Graaf FR, Schuijf JD, van Velzen JE, et al. Diagnostic accuracy of 320 -row multidetector computed tomography coronary angiography to noninvasively assess in-stent restenosis. Investigative radiology. 2010; 45(6):331–40. [PubMed: 20404736]
36. Chao SP, Law WY, Kuo CJ, et al. The diagnostic accuracy of 256-row computed tomographic angiography compared with invasive coronary angiography in patients with suspected coronary artery disease. European heart journal. 2010; 31(15):1916–23. [PubMed: 20233790]
37. Schoepf UJ, Zwerner PL, Savino G, Herzog C, Kerl JM, Costello P. Coronary CT angiography. Radiology. 2007; 244(1):48–63. [PubMed: 17495176]
38. Liu X, Zhao X, Huang J, et al. Comparison of 3D free-breathing coronary MR angiography and 64-MDCT angiography for detection of coronary stenosis in patients with high calcium scores. AJR Am J Roentgenol. 2007; 189(6):1326–32. [PubMed: 18029867]
39. Gharib AM, Ho VB, Rosing DR, et al. Coronary artery anomalies and variants: technical feasibility of assessment with coronary MR angiography at 3 T. Radiology. 2008; 247(1):220–7. [PubMed: 18372470]
40. Stuber M, Botnar RM, Danias PG, Kissinger KV, Manning WJ. Submillimeter three-dimensional coronary MR angiography with real-time navigator correction: comparison of navigator locations. Radiology. 1999; 212(2):579–87. [PubMed: 10429721]
41. Danias PG, McConnell MV, Khasgiwala VC, Chuang ML, Edelman RR, Manning WJ. Prospective navigator correction of image position for coronary MR angiography. Radiology. 1997; 203(3):733–6. [PubMed: 9169696]
42. Meyer CH, Pauly JM, Macovski A, Nishimura DG. Simultaneous spatial and spectral selective excitation. Magn Reson Med. 1990; 15(2):287–304. [PubMed: 2392053]
43. Wang Y, Ehman RL. Retrospective adaptive motion correction for navigator-gated 3D coronary MR angiography. J Magn Reson Imaging. 2000; 11(2):208–14. [PubMed: 10713956]

44. Stuber M, Botnar RM, Spuentrup E, Kissinger KV, Manning WJ. Three-dimensional high-resolution fast spin-echo coronary magnetic resonance angiography. Magn Reson Med. 2001; 45(2):206–11. [PubMed: 11180427]
45. Malayeri AA, Macedo R, Li D, et al. Coronary vessel wall evaluation by magnetic resonance imaging in the multi-ethnic study of atherosclerosis: determinants of image quality. J Comput Assist Tomogr. 2009; 33(1):1–7. [PubMed: 19188777]
46. Botnar RM, Stuber M, Danias PG, Kissinger KV, Manning WJ. Improved coronary artery definition with T2-weighted, free-breathing, three-dimensional coronary MRA. Circulation. 1999; 99(24):3139–48. [PubMed: 10377077]
47. Scott AD, Keegan J, Mohiaddin RH, Firmin DN. Noninvasive detection of coronary artery wall thickening with age in healthy subjects using high resolution MRI with beat-to-beat respiratory motion correction. J Magn Reson Imaging. 2011; 34(4):824–30. [PubMed: 21800396]
48. Herzog C, Arning-Erb M, Zangos S, et al. Multi-detector row CT coronary angiography: influence of reconstruction technique and heart rate on image quality. Radiology. 2006; 238(1):75–86. [PubMed: 16373760]
49. Austen WG, Edwards JE, Frye RL, et al. A reporting system on patients evaluated for coronary artery disease. Report of the Ad Hoc Committee for Grading of Coronary Artery Disease, Council on Cardiovascular Surgery, American Heart Association. Circulation. 1975; 51(4 Suppl):5–40. [PubMed: 1116248]

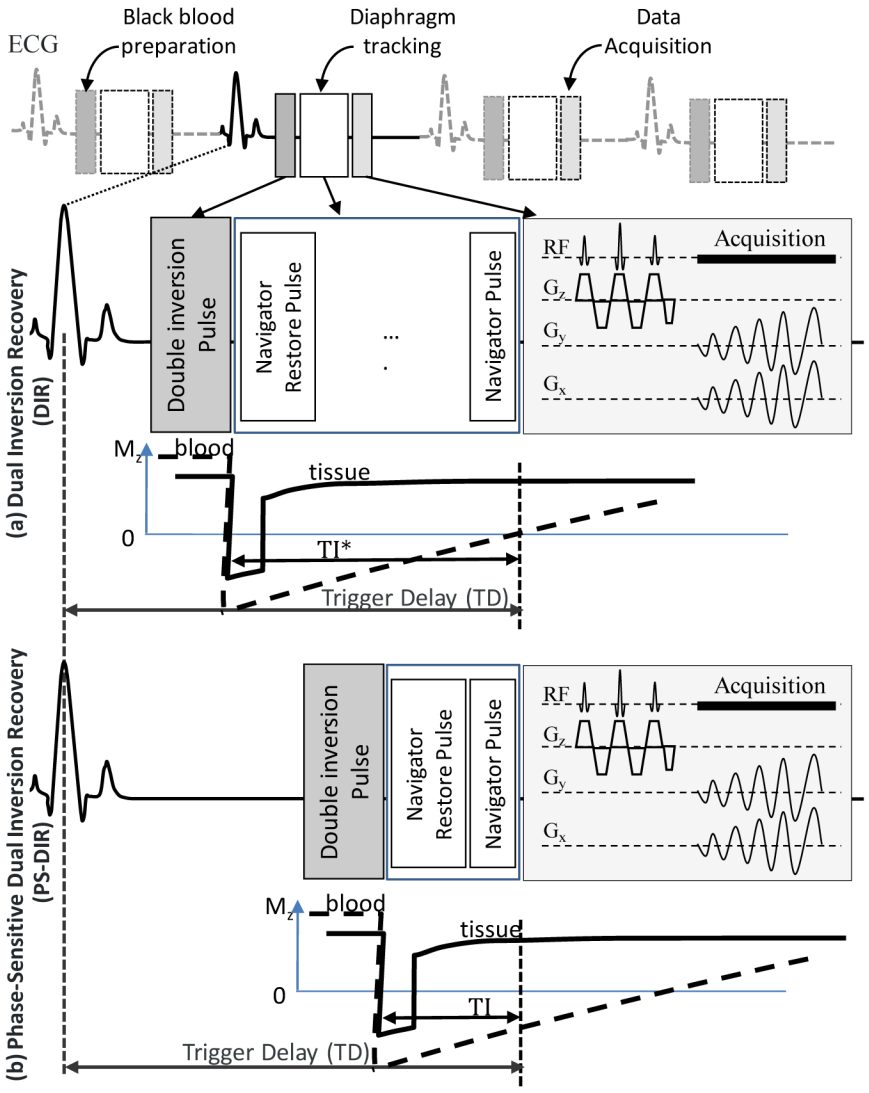

Figure 1.

The sequence diagram for free-breathing navigator-guided PS-DIR utilizing 2D spiral imaging of the coronary vessel wall with double inversion recovery black blood preparation and phase-sensitive lumen reconstruction. Every cardiac cycle the black blood preparation is directly followed by a navigator-restore pulse to restore the inverted magnetization at the navigator site. A navigator signal is acquired before data acquisition to accept or reject data. Data acquisition starts at the subject-specific rest period trigger delay (TD) using the water-selective pulse followed by a single shot spiral interleaf.

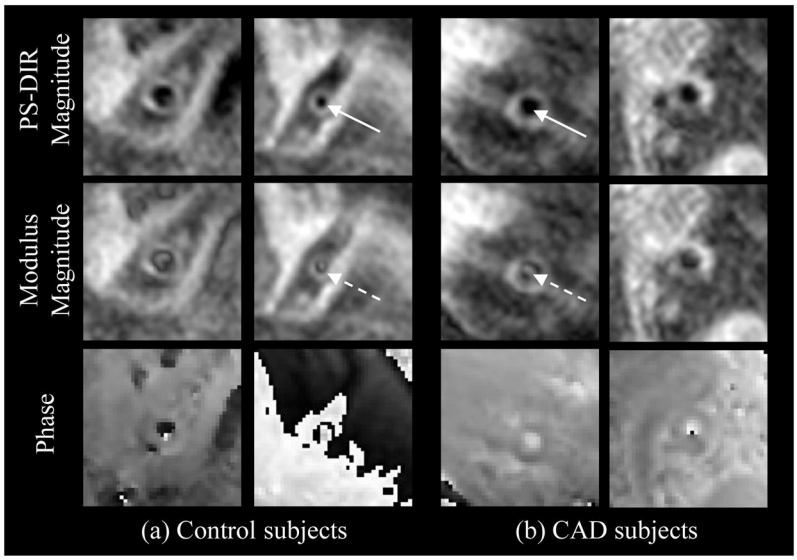

Figure 2.
Coronary arterial wall PS-DIR images of healthy and CAD subjects. Signed-magnitude PS-DIR reconstruction (top row) successfully restores lumen-wall contrast. The bright artifact signals in the middle of arterial lumen (middle row, broken arrows) were successfully suppressed using the phase information (bottom row) during reconstruction of the PS-DIR images (solid arrows).

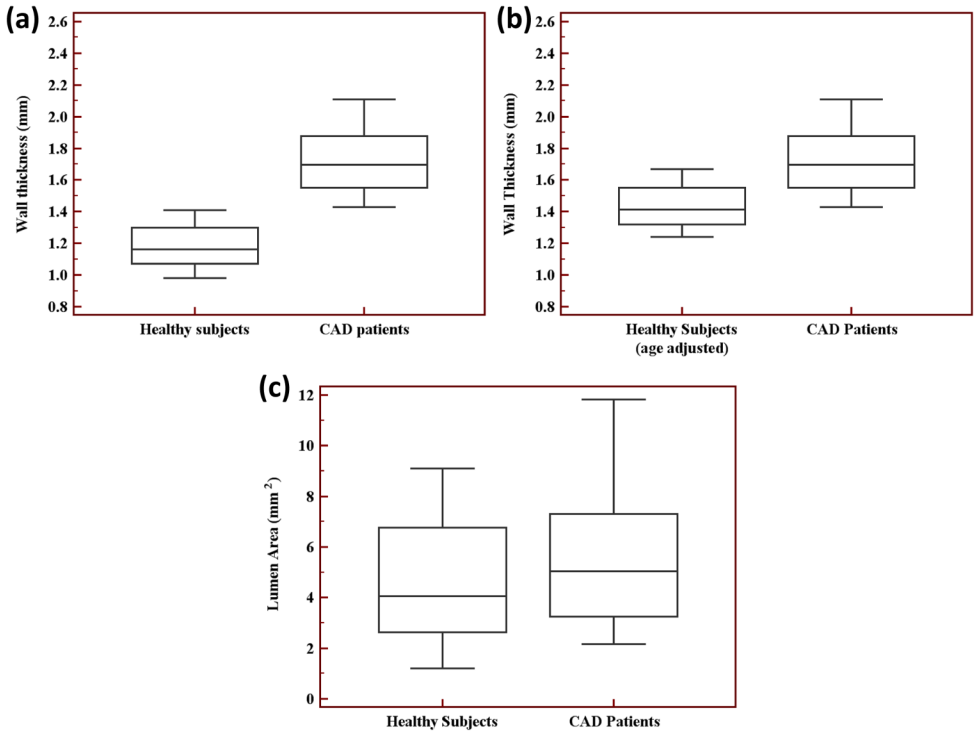

Figure 3.

Healthy subjects and CAD patients' box-and-whisker diagrams of the right coronary artery (a) vessel wall thickness, (b) vessel wall thickness with the healthy subjects' measurements adjusted for age, and (c) lumen area.

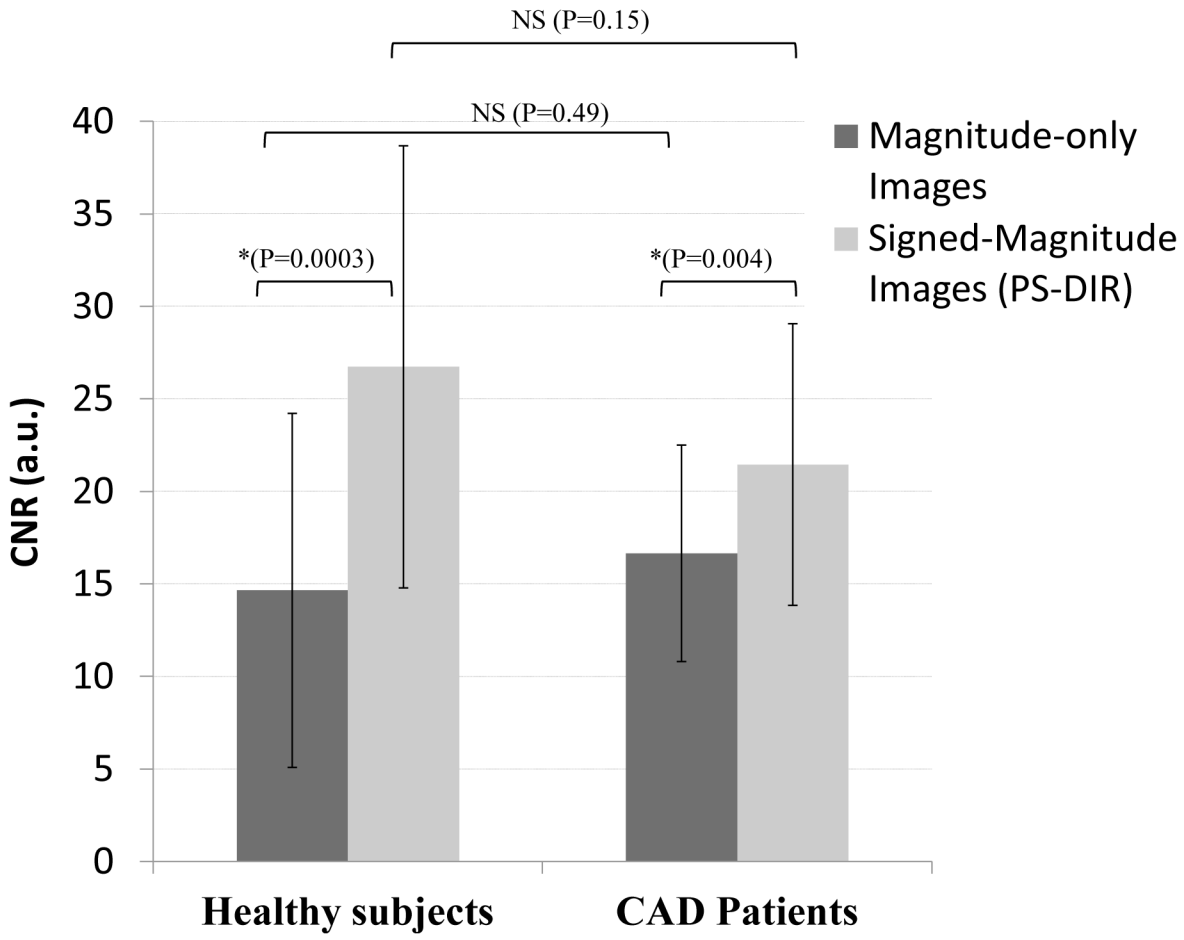

Figure 4.
Coronary wall thickness and area in CAD patients vs. healthy subjects. Results represent mean values ± 1 standard deviation.

Magn Reson Imaging. Author manuscript; available in PMC 2014 September 01.

Table 1

Demographics of the patients with risk factors and cardiac CT (CTA) findings. Risk factors included hypertension (HTN), family history (FH), dyslipidemia (DL), smoking (SH), prior myocardial infarction (MI) and diabetes mellitus (DM).

Age	Gender	Risk Factors	All Diseased Coronary Segments on CTA	Segments on CTA with >50% stenosis	Agatston Score
44	Female	HTN, DL, FH, SH	1,2,3,5,6,7,11,13	2,5,6,11,13	709
71	Female	HTN, FH, SH	1,2, 5,6,7,9,11	1,2,6,7,11	610.35
69	Female	DL, FH, SH	2,3,8,11		34.4
50	Male	HTN, DL, FH, SH	1,2,3,5,6,7,8,9,10,11	7,9,11	169.3
69	Male	HTN, DL, SH	1,5,6,7,9,11	7,9	610.6
46	Female	HTN, DM, DL, FH	1,2,5,7,9,11		0
72	Female	DL, SH	1,2,5,6,7,8,9,11	6,7,11	219
60	Male	HTN, DM, DL	1,5,6,7,8,9,10,11,13	6,7,10	1395.8
53	Female	HTN, DL, SH, FH	1,2,6,8,9,11	8	0
59	Female	HTN, DL	2,6,7,11,13	7	32.98
66	Female	HTN, DL, FH,	1,6		0
53	Female	HTN, DM, DL, FH	1,2,6,7,9,11		89.9
56	Female	DL	1,7,11		0
50	Male	HTN, DL, FH	2,6,7,11		0
60	Female	HTN	1,6,11		0
62	Male	HTN, FH, SH	1,2,3,5,6,7,8,11,13	1,2,3,6,7,8,11,13	2453.6
33	Male	HTN	6,7		43
65	Female	HTN, DL, FH	1,3,5,6,7,8,11,13	1,3,6,7,8,11,13	224.7
74	Male	HTN	1,5,6,7,8,11	5,6,7,8	258.1
52	Male	DL, SH	1,3,7,8,9,10		0
63	Male	HTN, SH	1,2,3,5,7,8,9,11	2,3,9	131.13

Table 2

Image quality scores in the healthy subjects and CAD patients involved in the study.

Score	Healthy subjects n(%)	CAD patients n(%)
4 “excellent”	9 (56.25%)	12 (57.14%)
3 “good”	5 (31.25%)	4 (19.05%)
2 “fair”	1 (6.25%)	1 (7.76%)
1 “poor”	1 (6.25%)	4 (19.05%)
0 “undistinguishable”	0	0

Table 3

Comparison of vessel geometrical properties and image quality between healthy subjects and CAD patients. Results in the table represent mean values ± 1 standard deviation.

Parameter	Healthy subjects	CAD patients	p value (healthy vs. patients)
Lumen area	4.51±2.42 mm^2	5.71±3.11 mm^2	0.25
Wall thickness	1.17±0.14 mm	1.74±0.27 mm	<0.0001*
Wall thickness (age-adjusted)	1.42±0.14 mm	1.74±0.27 mm	<0.001*
Wall area	12.75±2.79 mm^2	24.10±7.53 mm^2	<0.0001*
Outer wall area	17.26±4.77 mm^2	29.82±9.88 mm^2	0.0002*
W/OW	0.75±0.08	0.82±0.06	0.023*

* a significant difference ($p<0.05$).